Pergamon

Cement and Concrete Research 31 (2001) 363–373

CEMENT AND CONCRETE RESEARCH

Condition monitoring of deteriorating concrete dams using radar

Hong C. Rhim*

Department of Architectural Engineering, Yonsei University, Seoul 120-749, South Korea

Received 27 June 1999; accepted 4 December 2000

Abstract

Remote monitoring of the deterioration process of concrete dams has been studied by using radar to measure laboratory-size concrete specimens. The specimens represent five different physical conditions of deteriorating concrete dams. The investigation includes the manufacturing and the radar measurements of the specimens, and the implementation of signal processing schemes for generating two- and three-dimensional imagery of the specimens. The change in the radar signals that resulted from the specimens is related to the condition change inside the concrete. The results have shown the feasibility of using radar for monitoring the condition change inside concrete dams from a distance. © 2001 Elsevier Science Ltd. All rights reserved.

Keywords: Nondestructive testing; Aging; Degradation; Electrical properties; Image analysis

1. Introduction

Deterioration in concrete severely affects the service life, safety, and maintenance costs of concrete structures. Cracking, in particular, is one of the major factors contributing to the deterioration of concrete. Cracks exist in concrete even before the structure is subjected to any external loading. An excessive water–cement ratio, improper curing, and creation of high temperature during the hardening process may result in shrinkage, which is the direct cause of cracking. This is especially critical for large concrete structures such as dams due to the placement of massive concrete during construction. Those cracks, which exist in concrete at early stages, later expand and widen during service conditions after hardening. The intrusion of moisture contributes to crack propagation. This deterioration is further accelerated by freeze and thaw cycles and hydraulic fracture due to the presence of water. Deterioration mechanisms in concrete systems also include the failure of interfacing between concrete and other materials, and the fracture of concrete due to the excessive tensile stresses that arise from a corrosion of steel reinforcement. The focus of discussion in this paper is on the condition monitoring of concrete dams, which have no steel reinforcement.

Demand for the development of reliable nondestructive testing (NDT) techniques for concrete structures is ever increasing due to the growing concern about the deteriorating condition of infrastructures worldwide [1]. In 1984, some 2900 nonfederal dams in the United States were declared unsafe [2]. There are numerous examples of sudden and complete failure of dams while in service or failures of substructures of dams, such as gates, valves, and piers [3]. Effective NDT techniques are needed in order to assess the condition of existing concrete dams accurately before any replacement or rehabilitation action are taken. Inspections of dams are made at intervals dependent on dam classification, but they are usually done at least every 2 years. These inspections are generally limited to a surface examination of the dam, but may involve core sampling and concrete testing as well [4].

Up to the present, the radar method has generally been applied to the NDT of bridge decks and pavements in the infrastructure [5–7] in combination with other NDT methods. There have been exploratory studies on the viability of the radar method for NDT of the structural elements of concrete structures [8–10]. However, the technology is still too premature for the radar method to be used for massive concrete structures such as large dams. The probing of concrete dams requires a high-performance radar system and sophisticated problem-solving approaches. The success of the radar method as an NDT technique for concrete dams depends on the development of proper hardware and soft-

* Tel.: +82-2-548-5959; fax: +82-2-547-1853.
E-mail address: hcrhim@yonsei.ac.kr (H.C. Rhim).

PII: S0008-8846(00)00496-8

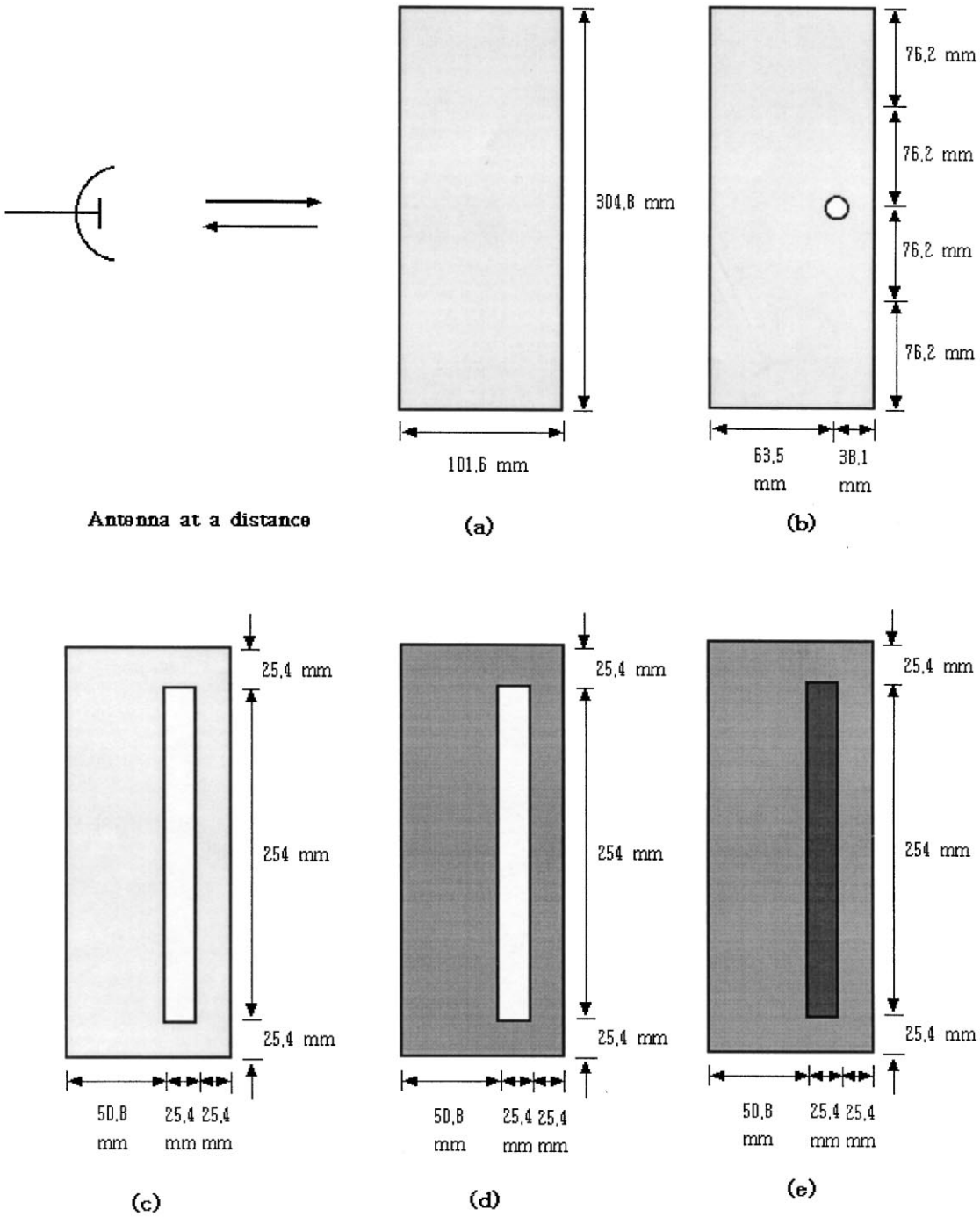

Fig. 1. Five concrete specimens representing five deterioration states of a dam. Dimensions of width and depth are shown. All specimens are 304.8 mm in height.

ware systems. It is also essential to view concrete as a material with electromagnetic properties and to study electromagnetic wave propagation through concrete [11]. The technique presented in this paper is intended to serve as a valuable aid in the inspection of concrete dams.

In this paper, the feasibility of using radar for the NDT of concrete dams is examined through radar measurements of laboratory size concrete specimens.

2. Deterioration scenario of a dam and concrete models

A concrete dam can have variable thickness and is always in contact with water on one side, while the other is usually exposed to air. An initially sound concrete dam can develop cracks during its service life, as described earlier. These relatively small size cracks will eventually become wider and can develop into holes or delaminations.

To complicate the matter, the intrusion of water from one side of a dam will moisturize the dam and eventually fill any cracks, holes, or delaminations inside the dam. Thus, enlarged cavities can form, presenting a safety problem for the dam.

In this work, it is suggested that, by using radar, such condition change in concrete dams can be detected. Radar transmits electromagnetic waves, which are reflected back whenever there is an impedance mismatch. Each material has its own impedance; for example, 1 is for air and 4–22 for concrete [10]. Thus, by examining this impedance mismatch, a boundary between different materials or an inclusion within a body can be detected using radar. As the sensitivity of a radar system increases, any small change in impedance can be discriminated. However, as an energy loss occurs during the travel of the electromagnetic waves inside a material, such as concrete, detection capability is in reality limited.

To investigate the detectability of such condition change inside a dam, a simplified deterioration scenario is established as a basis for measuring the difference in response between defective and sound concrete. The deterioration scenario is given as follows: (i) there exists a sound concrete dam, which is represented by a 304.8 mm (width) × 304.8 mm (height) × 101.6 mm (thickness) dry plain concrete block model in Fig. 1a; (ii) a hole created inside the concrete represents the onset of deterioration in Fig. 1b; (iii) a delamination is developed inside the dam, which is represented by a 254 mm (W) × 304.8 mm (H) × 25.4 mm (D) delamination at a 50.8 mm depth from the surface of the block in Fig. 1c; (iv) the dam is now moisturized due to the intrusion of water, which is represented by a wet concrete block having the same delamination filled with air in Fig. 1d; and, finally, (v) the delamination is filled with water over a period of time inside the wet concrete in Fig. 1e.

Physical states of concrete specimens corresponding to each step in the deterioration scenario are illustrated in Fig. 1. Five concrete specimens, which represent each step of the deterioration, are manufactured for radar measurements. The specimens were cast with a water/cement/sand/coarse aggregate mix ratio of 1:2.22:5.61:7.12 (by weight). Type I portland cement was used. Coarse aggregates had a maximum size of 38.1 mm. After being cast, the hardened concrete specimen was placed into water for 7 days for curing. Depending on the measurement condition, dry specimens were air-dried in ambient temperature and humidity, while wet specimens were placed in water for 2 months before the measurements. The uniaxial compression strength of the dry specimen was 21 MPa at 28 days. Radar measurements were made 2 months after casting. Specimens 1d and 1e in Fig. 1 were submerged into water for 2 months prior to measurements to ensure that the entire specimen was moisturized. Water was taken out of the delamination from specimen 1d in Fig. 1 to have solely air-filled delamination, while the delamination inside specimen 1e in Fig. 1 was filled with water before the measurement.

3. Use of radar and measurement setup

The use of radar to monitor condition change inside concrete dams or specimens is based on the principle that, at the boundary between two media, an impedance mismatch occurs causing part of the energy to be reflected from the material and the rest of the energy to be transmitted through the material. This interaction permits a nondestructive inspection of the material's interior for property determination and the detection of anomalies. The mathematical expressions of the reflected wave can be written as (Eq. (1))

$$R_{\mathrm{TE}} = \frac{\sqrt{\varepsilon_{r1}}\cos\theta_{\mathrm{i}} - \sqrt{\varepsilon_{r2}}\cos\theta_{\mathrm{t}}}{\sqrt{\varepsilon_{r1}}\cos\theta_{\mathrm{i}} + \sqrt{\varepsilon_{r2}}\cos\theta_{\mathrm{t}}} \tag{1}$$

where R_{TE} is the reflection coefficient for perpendicular polarization or Transverse Electric (TE). ε_{r1} is the dielectric constant for medium 1 (for air, $\varepsilon_{r1}=1$), ε_{r2} is the dielectric constant for medium 2 (for concrete, $\varepsilon_{r2}=4-22$), θ_{i} is the angle of incidence, and θ_{t} is the angle of transmission, as shown in Fig. 2.

A radar system used for the measurements generates a stepped frequency gated continuous wave, which sweeps frequency from starting frequency to ending frequency by a

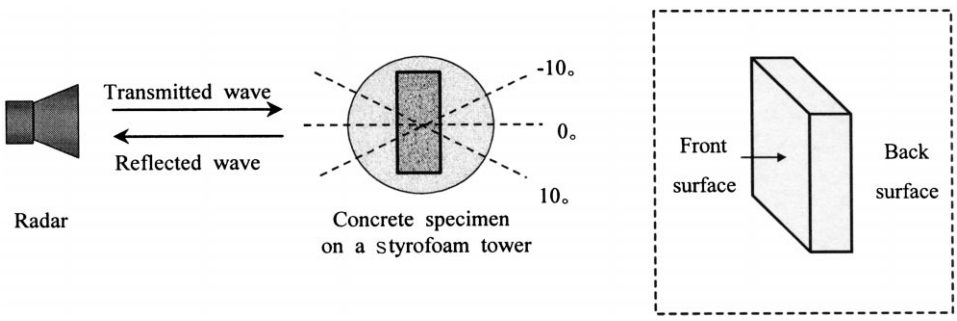

Fig. 2. Radar measurement setup.

given increment at an incident angle. In this work, the frequency range was from 3.4 to 5.8 GHz with an increment of 0.1 GHz. This gave a range resolution of 62.5 mm in air and improved resolution inside dry and wet concrete specimens based on Eq. (2):

$$\rho_r \text{ in concrete} = \frac{\left(\frac{c}{\sqrt{\varepsilon_r}}\right)}{2B} \tag{2}$$

where ρ_r is the range resolution, c is the speed of light ($c = 3.0 \times 10^8$ m/s), ε_r is the dielectric constant of concrete, and B is the frequency bandwidth of incident waves. The range resolution is the ability to distinguish between closely spaced objects in the direction of wave propagation. The dielectric constant is a real part of a complex permittivity, which determines how much electromagnetic energy is stored. For dry and wet concrete specimens, the dielectric constants are known to be 4.5 and 8 in the 3.4–5.8 GHz frequency range, respectively [10]. These values give a resolution of 29.5 mm for dry concrete specimens and 22.1 mm for wet ones, respectively. The specimen is placed vertically as a target at the top of a styrofoam tower (Fig. 3). The radar is located 14.4 m away.

The incident wave generated by the antenna of an Inverse Synthetic Aperture Radar (ISAR) system is a stepped frequency continuous wave. It has a pulsewidth of 20 ns and power of 30 dBm. The antenna transmits the waves from a starting frequency of f_1 to an ending frequency of f_2 by a frequency increment of 0.1 GHz. Thus, the frequency is swept from f_1 to f_2 at different time steps.

The purpose of using ISAR is to generate crossrange imagery. ISAR techniques have been used to produce target images for objects on rotating platforms, for satellites rotating in orbit, and even for ships at sea, which roll rhythmically on the sea surface [12]. There are three major measurement parameters to be considered prior to ISAR measurements: center frequency (f_c), the frequency bandwidth (B) of incident waves, and the rotational angle $\Delta\theta_{rad}$ of a target. These three parameters determine range and crossrange resolutions. The crossrange resolution, ρ_{xr} is determined by Eq. (3):

$$\rho_{xr} \text{ in concrete} = \frac{\left(\frac{c}{f_c\sqrt{\varepsilon_r}}\right)}{2(\Delta\theta_{rad})} \tag{3}$$

The crossrange resolution is an ability to distinguish between closely spaced objects in the direction perpendicular to the direction of wave propagation.

4. Signal processing scheme

Upon radar measurements of concrete specimens, sets of raw data are collected, which contain information on the returned signals from the concrete targets. By processing the raw data, one- and two-dimensional imagery can be obtained.

The reflected wave is collected in frequency by the same antenna. The measured data have information on aspect angle, frequency, and amplitude (Table 1). Each entry in the

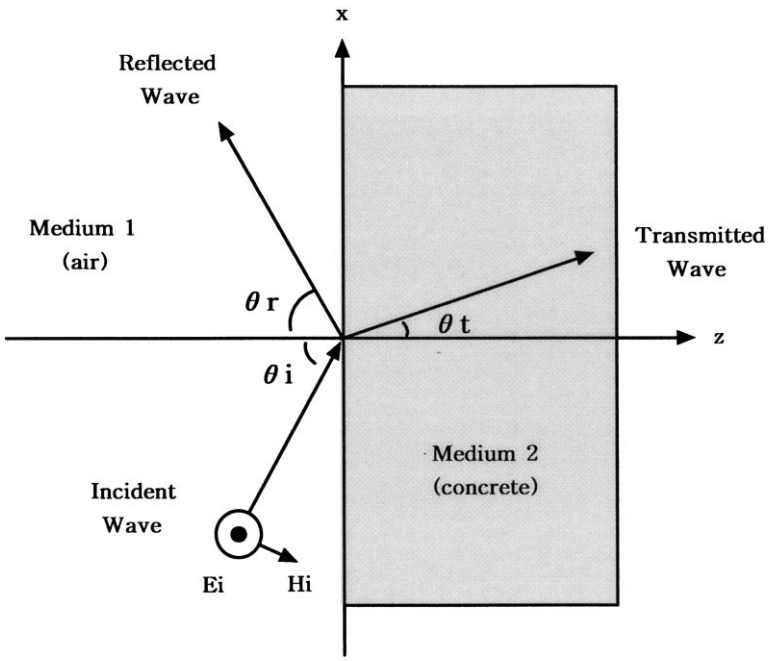

Fig. 3. Reflection and transmission of a perpendicular-polarized (TE) plane wave at a dielectric boundary shown on the x–z plane (the plane of incidence). The electric field E is in the y direction.

Table 1
A sample data from ISAR measurements

		VV polarization		HH polarization	
Aspect angle (°)	Frequency (MHz)	Amplitude (dBsm)	Phase (°)	Amplitude (dBsm)	Phase (°)
0.00	3400	− 9.84	− 88.91	− 9.67	− 82.23
0.00	3500	− 9.69	− 71.39	− 9.11	− 68.10
0.00	3600	− 9.34	− 54.21	− 9.06	− 54.16
0.00	...	...	...	...	...
0.00	5800	− 8.46	26.47	− 8.37	29.19

data records the amplitude and phase change of the signal received at each frequency.

To generate one-dimensional imagery, sweeping frequency measurements are made at a normal incident angle.

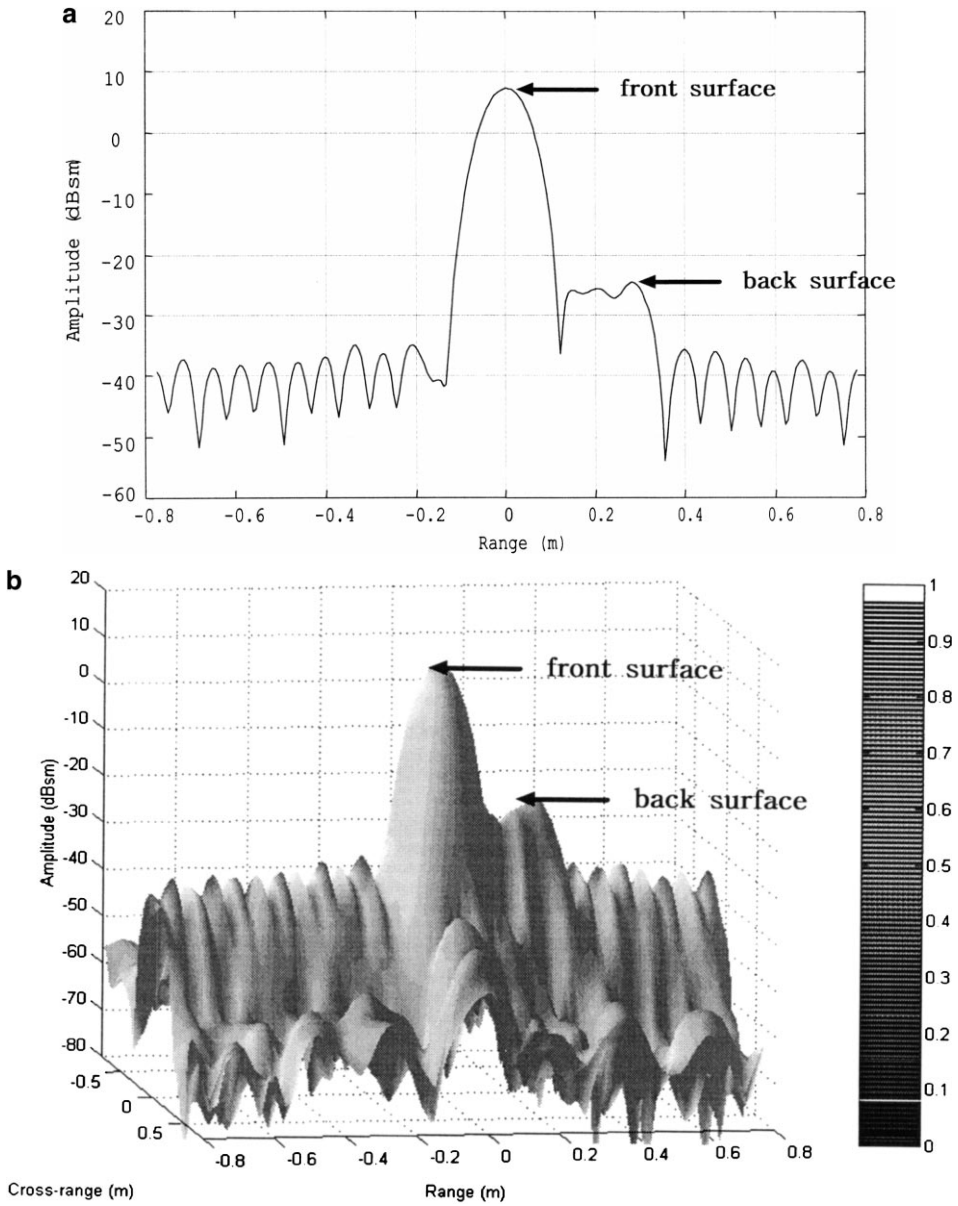

Fig. 4. (a) Two-dimensional plot of the 1D measurements of a 304.8 × 304.8 × 101.6 mm dry concrete block at 3.4–5.8 GHz. (b) Three-dimensional plot of the 2D measurements of a 304.8 × 304.8 × 101.6 mm dry concrete block at 3.4–5.8 GHz.

To generate two-dimensional imagery, sweeping frequency measurements are made from -10° to $+10^\circ$ angles. In both cases, the received signals in frequency are multiplied by a window function and then inverse Fourier transformed to obtain an image in a time domain [13].

5. Results and discussion

Results of radar measurements on five concrete models are presented in Figs. 4–8. In all figures, two-dimensional images are shown in part a of the figures, and three-dimensional images are shown in part b of the figures, respectively. The imagery obtained by radar is different from that seen by human eyes. By rotating the specimen for 20 degrees while using the ISAR, three-dimensional imagery is generated, as in part b of the figures. Three-dimensional figures provide the overall imagery. Two-dimensional figures are made by selecting data at a 0° incident angle. Thus, normal incident angle measurements are shown in part a of the figures.

In Fig. 4, sound plain concrete is imaged. The front surface is clearly seen in both Fig. 4a and b. The magnitude of the lobe (peak) from the front surface is much higher than that of the lobe from the back surface, as there is much attenuation of the waves traveling through the 101.6-mm

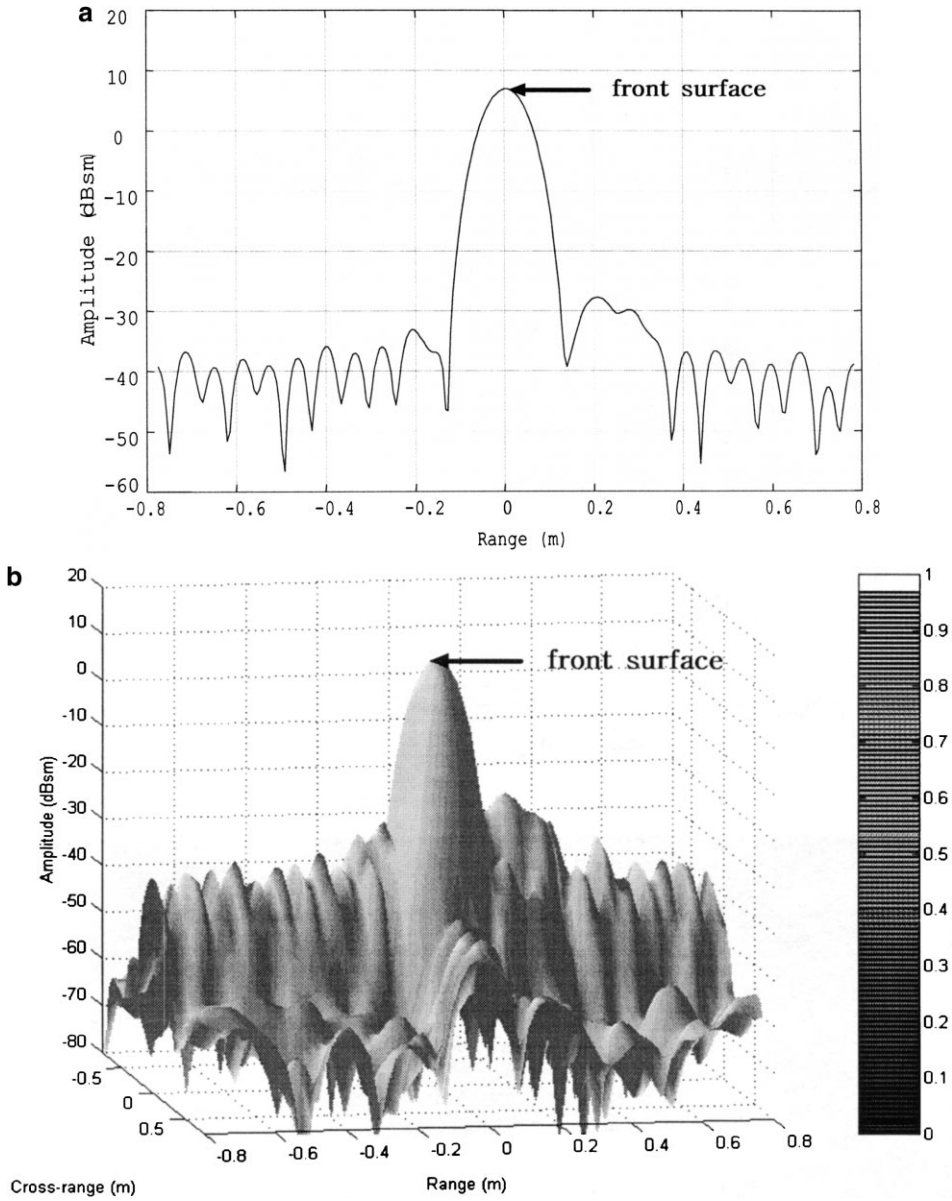

Fig. 5. (a) Two-dimensional plot of the 1D measurements of a 304.8 × 304.8 × 101.6 mm dry concrete block with three 12.7-mm-diameter holes at a depth of 50.8 mm. (b) Three-dimensional plot of the 2D measurements of a 304.8 × 304.8 × 101.6 mm dry concrete block with three 12.7-mm-diameter holes at a depth of 25.4 mm.

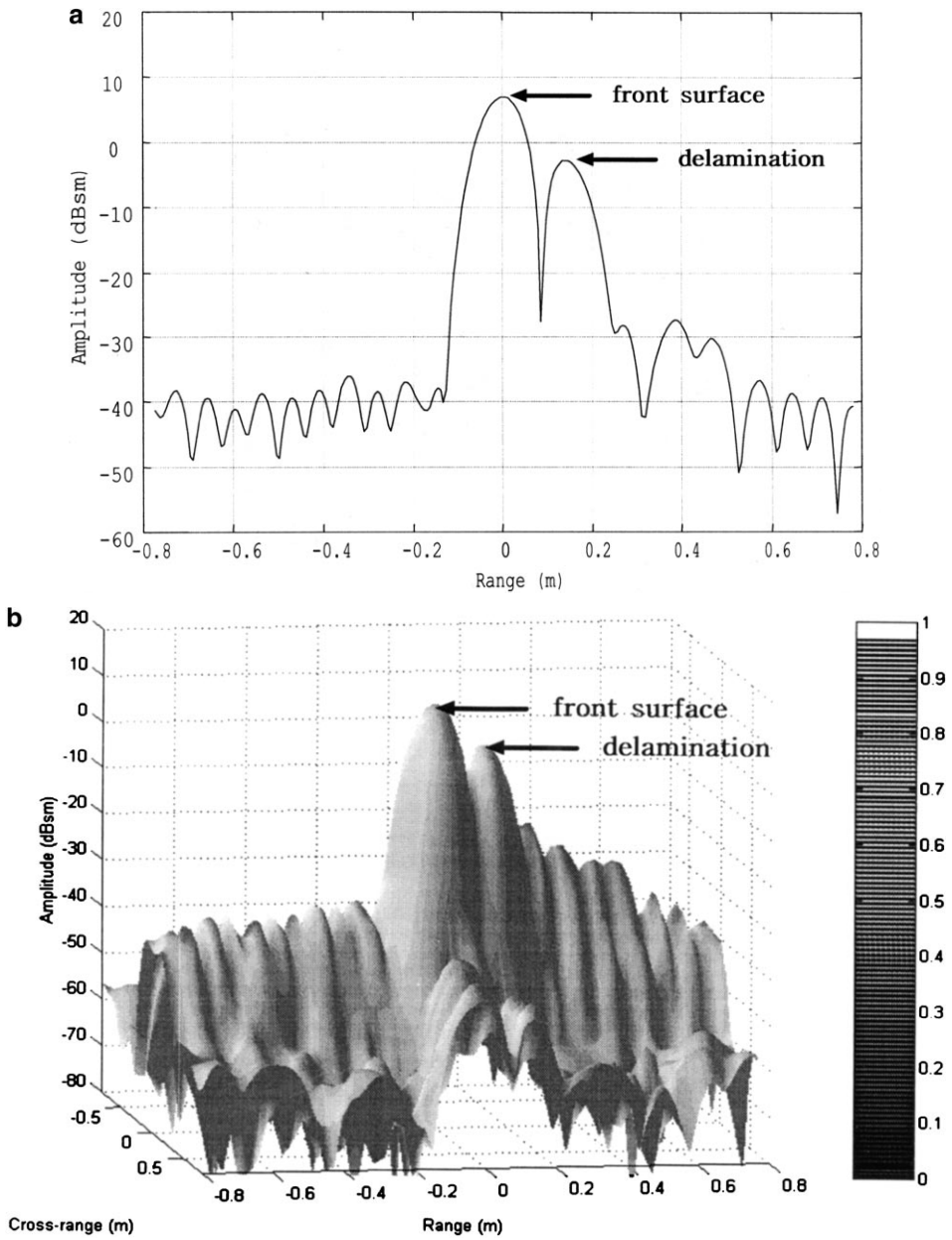

Fig. 6. (a) Two-dimensional plot of the 1D measurements of a 304.8 × 304.8 × 101.6 mm dry concrete block with a 25.4-mm-thick delamination at a depth of 50.8 mm. (b) Three-dimensional plot of the 2D measurements of a 304.8 × 304.8 × 101.6 mm dry concrete block with a 1-in.-thick delamination at a depth of 2 in.

thickness of the specimen. The frequency range of 3.4–5.8 GHz is adequate for concrete thickness detection and condition change monitoring. Small lobes in the −0.8 to +0.8 m range are due to noise from radar measurements and signal processing. As this noise level increases, it becomes difficult to identify the reflections from the boundaries of the two different media.

A change in the returned signal is noticed in Fig. 5. The peak corresponding to back surface near 0.28 m in the range direction in Fig. 4a is now disappeared in Fig. 5a. Due to its small size, the initiation of a 12.7 mm diameter hole is not great enough to be detected. However, the reflected signal is changed from Fig. 4, an alarm that marks the beginning of the deterioration process. Any NDT method has its range for optimum detection. It depends on the physical condition of the target, as well as the sensitivity of the measurement system. With the radar measurement set-up used in this experiment, it is possible to detect condition change. This finding of difference in returned signal is quite feasible as long as there are reference data available.

In Fig. 6, as the hole is widened and becomes delaminated, the existence and location of the delamination is positively identified. This distinct appearance of the delamination peak is due to the great reflection coefficient at the

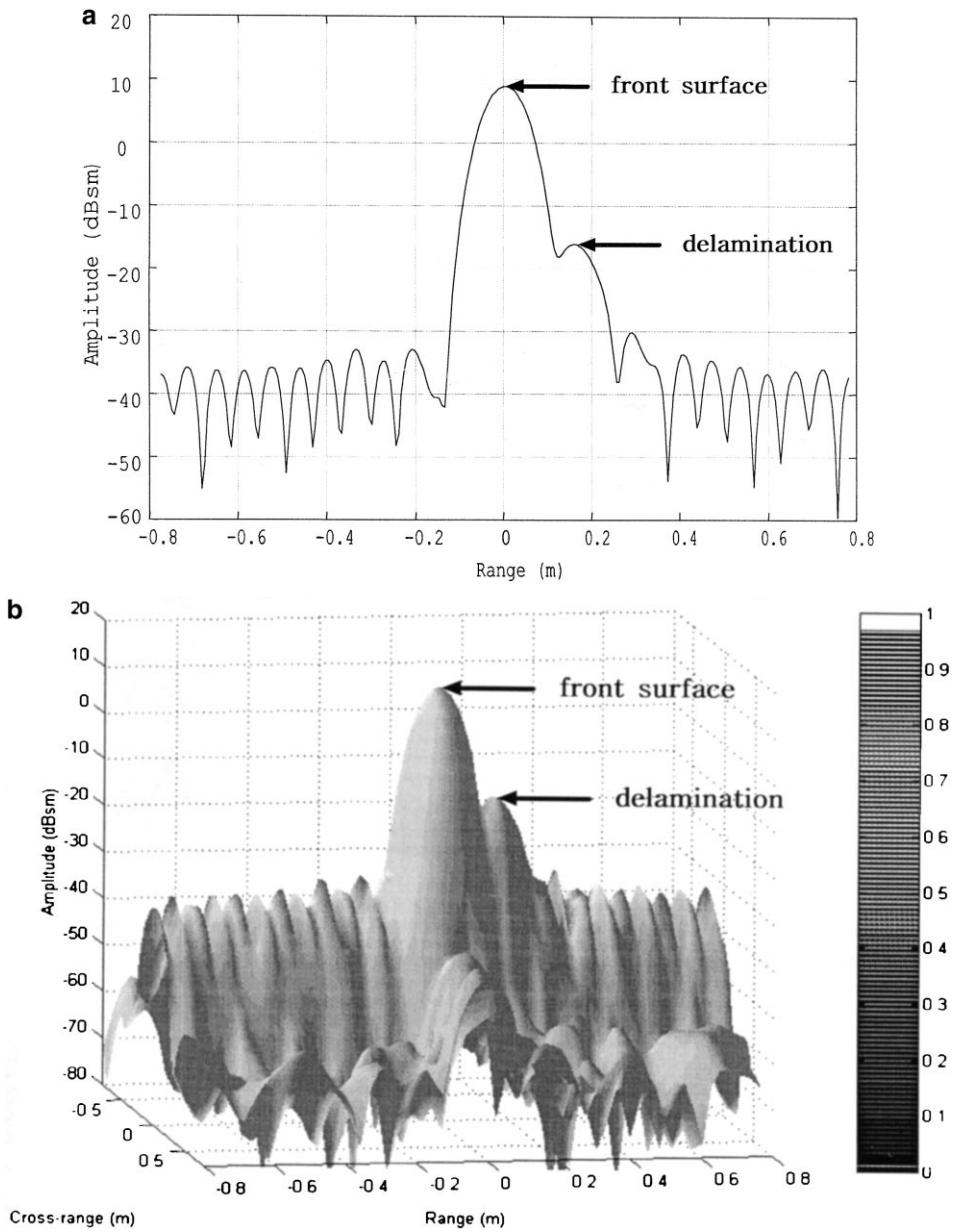

Fig. 7. (a) Two-dimensional plot of the 1D measurements of a 304.8 × 304.8 × 101.6 mm wet concrete block with a 25.4-mm-thick delamination at a depth of 50.8 mm. (b) Three-dimensional plot of the 2D measurements of a 304.8 × 304.8 × 101.6 mm wet concrete block with a 25.4-mm-thick delamination at a depth of 50.8 mm.

concrete/air boundary at the beginning of the delamination. In Fig. 6a and b, the second peak is smaller than the first peak from the front surface of the concrete. There are also some changes in the smaller lobes in addition to the front surface and delamination in Fig. 6. The reflected signals are disturbed as the wave propagation and reflection pattern become more complicated in the sound concrete; this means that there is an inclusion.

After the moisturization of the concrete block, reflection from the delamination decreases due to the increased loss in the wet block. This phenomenon is shown as a decreased peak in Fig. 7. This illustrates the difficulty of detecting objects inside wet concrete. The detection of a water-filled delamination is not possible quantitatively, but it is possible qualitatively. The propagation of electromagnetic waves is governed by Maxwell's equations. A plane wave propagation along a z direction (Fig. 3) is of the form [14]

$$\bar{E} = \hat{y} E_0 \mathrm{e}^{-jk_z^* z + j\omega t} \tag{4}$$

where $\bar{E}$ is the electric field vector, $\hat{y}$ is a unit vector in the y direction, which is perpendicular to the direction of wave propagation (or it can be $\hat{x}$ if in the x direction), is the initial amplitude of the wave's electric field, and $k_z * z$ is the complex wavenumber in the z direction. If only the spatial term in Eq. (4) is considered and the complex

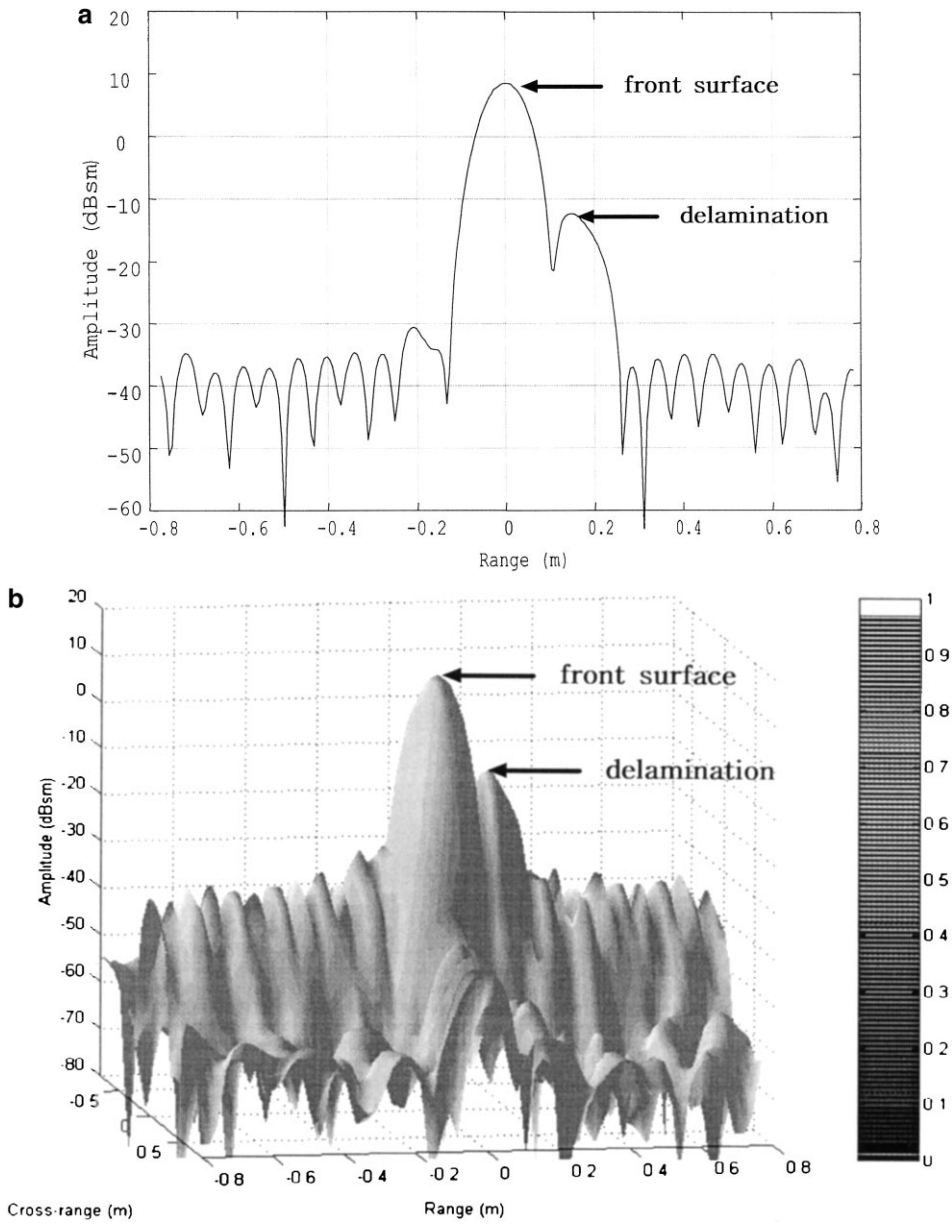

Fig. 8. (a) Two-dimensional plot of the 1D measurements of a 304.8 × 304.8 × 101.6 mm wet concrete block with a 25.4-mm-thick delamination filled with water at a depth of 50.8 mm. (b) Three-dimensional plot of the 2D measurements of a 304.8 × 304.8 × 101.6 mm wet concrete block with a 25.4-mm-thick delamination filled with water at a depth of 50.8 mm.

wavenumber is replaced with its real and imaginary parts, Eq. (4) becomes

$$\bar{E} \propto e^{-jk_z^* z} \tag{5}$$

$$\bar{E} \propto e^{-jk_z' z} e^{-k_z'' z}$$

where $k_z^* z = k_z' z - jk_z z$. The second term [Eq. (5)] represents the amplitude loss of the electric field with distance (in the z direction) due to material attenuation. More concisely, Eq. (5) can be written as

$$E \propto e^{-k_z'' z} \tag{6}$$

if only considering amplitude loss. The loss is exponential in nature as k_z increases. k is the imaginary part of the complex wavenumber. For dielectric materials with low conductivity, it is approximated as [Eq. (7)]

$$k'' = \frac{\sigma}{2}\sqrt{\frac{\mu_0}{\varepsilon'}} \tag{7}$$

k is often termed as the attenuation coefficient. It determines the amplitude loss of the wave in a dielectric material and changes as a function of conductivity and the real part of the complex permittivity, which in turn changes as frequency changes. The significance of the

attenuation coefficient for nondestructive evaluation is that its inverse is a penetration depth of the wave in a dielectric medium.

As the last step in the deterioration scenario, the delamination is now filled with water. The delamination is visible again due to the strong reflection from the water filled inside the delamination in Fig. 8. Where the physical dimensions of the interface or anomaly are small, the target-scattering loss increases owing to the geometry of the situation, and the returned signal becomes smaller. Under some conditions, the physical dimensions of the anomaly are such as to create a resonant structure which increases the level of the return signal and decreases the target-scattering loss. It is possible to distinguish air-filled delaminations and water-filled delaminations by examination of their resonant characteristics and the relative phase of the reflected wavelet. Water has a relative dielectric constant of 81, which will serve to reduce the resonant frequency, and this variation may be the means of identifying water-filled delaminations.

Many of the targets being searched for by radar methods are nonmetallic, so their scattering cross-section is dependent on the properties of the surrounding dielectric medium. Where the relative permittivity of the target is lower than that of the surrounding medium, such as an air-filled delamination below concrete, the interface does not produce a phase reversal of the backscattered wave. Conversely, when the scattering is caused by a metallic boundary or where the relative permittivity of the target is larger than the surrounding medium, phase reversal occurs in the backscattered wave [15]. The physical shape of the target will influence the frequency and polarization of the backscattered wave, and can be used as a means of preferential detection. The effect of the high permittivity of moisturized concrete dam means that some targets, such as water-filled delaminations, produce a stronger radar return when buried than when in free space. In such circumstances, the radar is responding primarily to the dielectric properties of the enclosed volume (i.e., the water- or air-filled delamination).

When an obstacle is illuminated by an electromagnetic wave, energy is dispersed in all directions. The type of target being sought (i.e., a sphere, a linear target, or an interface) affects the choice of antenna type and configuration, as well as the kind of signal-processing techniques, which may be employed. In addition, the spatial distribution of energy depends on the size, shape, and composition of the obstacle, and on the frequency and nature of the incident wave [16]. As a result, the detectability of holes and delaminations can be determined by their size and location from surface. A concrete dam subject to deterioration can be monitored periodically by radar, with any changes in the returned signal indicating the presence of abnormalities. Similar applications of the method will effect a periodic quality control of existing structures.

6. Conclusion

This paper is directed towards the experimental verification of novel ideas concerning the use of radar in the condition monitoring of deteriorating concrete dams. The experiments are based on the principle that changes associated with a dielectric constant are shown in the reflected waves returning from concrete targets.

It is concluded that a condition monitoring of a concrete dam over a certain period is possible as described above because a change in the reflected signal represents a quality change inside the dam. Based on this principle, practical techniques can be developed for the condition monitoring of concrete dams and the detection of subsurface condition changes using radar.

Acknowledgments

This work was partially supported by the Korea Earthquake Engineering Research Center (KEERC) funded by the Korea Science and Engineering Foundation (KOSEF). Computational facilities were provided by the Advanced Building Science and Technology Research Center (ABSTRC) by the College of Engineering at Yonsei University.

The raw data from the ISAR measurement were obtained at the Department of Civil and Environmental Engineering at Massachusetts Institute of Technology and MIT Lincoln Laboratory through a research project supported by the US Army Corps of Engineers, Waterways Experiment Station, Vicksburg, MS through Contract No. DACW39-92-K-0029. The author would like to thank Prof. Oral Buyukozturk at MIT, Dr. Tony C. Liu, Mr. Mitch Alexander, and Mr. Kenneth Saucier at the US Army of Engineers for the support that they provided. Special thanks are due to Prof. Jin A. Kong of the Department of Electrical Engineering and Computer Science and to Dr. Robert T. Shin at MIT Lincoln Laboratory.

The author would also like to thank Mr. You Sok Kim of Nondestructive Evaluation and Structures Laboratory (NDESLAB) at Yonsei University for his help in preparing this paper through an internship provided by KOSEF.

References

[1] K.P. Chong, J.B. Scalzi, O.W. Dillon, Overview of nondestructive evaluation projects and initiative at NSF, J. Intell. Mater. Syst. Struct. 1 (1990) 422–431.
[2] American Society of Civil Engineers, Evaluation Procedures for Hydrologic Safety of Dams, ASCE, Virginia, 1988.
[3] A.O. Babb, T.W. Mermel, Catalog of Dam Disasters, Failures and Accidents, US Department of the Interior Bureau of Reclamation, Washington, DC, 1968.
[4] G.F. Cox, Dam safety in British Columbia, Proc. Dam Saf. Semin., (1986) 3–10.

[5] T. Chung, C.R. Carter, T. Masliwec, D.G. Manning, Impulse radar evaluation of asphalt-covered bridge decks, IEEE Trans. Aerosp. Electron. Syst. 28 (1) (1992) 125–137.
[6] U.B. Halabe, K. Maser, E. Kausel, Condition Assessment of Reinforced Concrete Structures Using Electromagnetic Waves, Technical Report to US Army Research Office, 1989.
[7] K.R. Maser, W.M.K. Roddis, Principles of thermography and radar for bridge deck assessment, J. Transp. Eng. 116 (5) (1990) 583–601.
[8] H.C. Rhim, O. Büyüköztürk, D.J. Blejer, Remote radar imaging of concrete slabs with and without a rebar, Mater. Eval. 53 (2) (1995) 295–299.
[9] J.H. Bungey, S.G. Millard, M.R. Shaw, Simulation tank to aid interpretation of radar results on concrete, Mag. Concr. Res. 45 (164) (1993) 187–195.
[10] H.C. Rhim, O. Büyüköztürk, Electromagnetic properties of concrete at microwave frequency range, ACI Mater. J. 95 (3) (1998) 262–271.
[11] O. Büyüköztürk, H.C. Rhim, Modeling of electromagnetic wave scattering by concrete specimens, Cem. Concr. Res. 25 (5) (1995) 1011–1022.
[12] J.L. Eaves, E.K. Reedy, Principles of Modern Radar, Van Nostrand-Reinhold, New York, 1987.
[13] H.C. Rhim, Nondestructive Evaluation of Concrete Using Wideband Microwave Technique, PhD Thesis, Department of Civil and Environmental Engineering, Massachusetts Institute of Technology, Cambridge, MA, 1995.
[14] J.A. Kong, Electromagnetic Wave Theory, second ed., Wiley, New York, 1990.
[15] D.J. Daniels, Surface-Penetrating Radar, The Institution of Electrical Engineers, UK, 1996.
[16] E.F. Knott, J.F. Shaeffer, M.T. Tuley, Radar Cross Section, Artech House, Dedham, MA, 1985.